

# Comparative tribological investigation of castor oil and its transesterified and aminolyzed derivatives

G. Lasch<sup>\*a</sup>, P. Stradolini<sup>b</sup>, G.S. Gehlen<sup>ac</sup>, L.Y. Barros<sup>a</sup>, J.C. Poletto<sup>ad</sup>, A. Ramalho<sup>e</sup>,  
C.M.C.G. Fernandes<sup>f</sup>, P. C. Romio<sup>f</sup>, C.L. Petzhold<sup>b</sup>, N.F. Ferreira<sup>a</sup>, P. D. Neis<sup>a</sup>

<sup>a</sup>Federal University of Rio Grande do Sul, Laboratory of Tribology, Sarmiento Leite 425 – Porto Alegre, Brazil

<sup>b</sup>Federal University of Rio Grande do Sul, Institute of Chemistry, Bento Gonçalves 9500 – Porto Alegre, Brazil

<sup>c</sup>Trento University, Department of Industrial Engineering, Via Sommarive 9, 38123 – Trento, Italy

<sup>d</sup>Ghent University, Soete Laboratory, Technologiepark Zwijnaarde 46, 9052, Zwijnaarde – Ghent, Belgium

<sup>e</sup>University of Coimbra, Department of Mechanical Engineering, CEMMPRE, Rua Luis Reis Santos, 3030-788 – Coimbra, Portugal

<sup>f</sup>FEUP, University of Porto, Rua Dr. Roberto Frias, 4200-465 – Porto, Portugal

Received Date Line (to be inserted by Production) (8 pt)

---

## Abstract

This study compared the tribological performance of castor oil (CO), its transesterified (TCO), and aminolyzed (ACO) forms. A limited number of research articles are available regarding the tribological properties of these modified forms, especially the aminolyzed. Assessments included film thickness, piezoviscosity, Stribeck curve, and scuffing resistance. The film thickness followed the same order of the dynamic viscosity, i.e.: CO > ACO > TCO. The chemical modifications reduced the piezoviscosity, which was estimated as following: CO > TCO > ACO. ACO exhibited the lowest coefficient of friction (CoF) in the mixed and boundary regimes. ACO with a strong adsorbed film and lower piezoviscosity (consequently stable viscosity and reduced heating) demonstrated superior tribological properties (higher scuffing resistance and lower CoF).

Keywords: Biolubricant; Castor oil; Coefficient of friction; Scuffing.

---

## 1. Introduction

Lubricants play a critical role in the proper functioning and maintenance of machinery and equipment across various industries. Traditionally, mineral and synthetic oil-based lubricants have been widely used due to their good lubricating properties. However, the use of those lubricants results in negative environmental impacts, as well as potential health risks [1,2]. As a result, there has been growing interest in the use of biolubricants, since they are derived from renewable resources, they are biodegradable [2,3], and have good lubricity and lower volatility than the mineral and synthetic ones [4]. Although biolubricants offer significant environmental and health benefits over the conventional (mineral and synthetic) lubricants, they are also known to have some drawbacks, as their low thermal and oxidative stability, i.e., low resistance to degradation [2]. This low resistance to degradation is related to considerable changes in viscosity with temperature, as well as undesirable oxidation processes [2,5–7]. Several techniques can enhance these undesirable traits, including modifying the fatty acid profile of vegetable oils genetically, modifying chemically the base oil or adding additives to it, such as antioxidants, viscosity modifiers and pour point depressants [2,8,9]. Of these techniques, chemical modification of the base oil stands out as the most promising, showing significant potential in enhancing chemical stability over a wide temperature range [2,9].

Chemical modification mainly involves the modifying of the acyl (C=O) and the alkoxy (O–R) functional groups. One example of chemical modification is transesterification. This process rearranges the acyl moieties to form new triesters from triglycerides. Different vegetable sources have been developed through transesterification like soybean [10,11], castor oil [12–16], karanja [17], rice bran [17], rape seed [14,18] and *Jatropha curcas* [18,19] for being used as biolubricants. However, few works have focused on

their tribological behavior or have done an in-depth analysis of the sliding performance of those chemically changed biolubricants. Aminolysis is another chemical modification that can be used to rearrange the acyl moieties by forming new amides from triglyceride. This process has been used in various applications, such as polymers [20,21], lubricant additives [22,23], adhesives [24] and biodiesel production [25,26]. Moreover, to the best of the authors knowledge, there is only one study where aminolysis is used to produce an aminolyzed base-oil [13]. However, in this study the researchers did not evaluate the tribological properties of the resulting biolubricant.

Among the vegetable oils, castor oil (CO) stands out as one of the most versatile and interesting option due to its high hydroxyl index, viscosity, low toxicity, biodegradability and it is not edible (i.e. it does not compete with production for food) [12–16]. Although castor oil seeds make up to only 3% of the global plant oil seed production, the extraction of non-edible castor oil is readily achievable from castor plants that flourish even in arid regions, such as Brazil [13,15].

Despite the existing research on castor oil (CO) [27] and transesterified castor oil (TCO) [12–16,28], still a complete tribological characterization of those oils is missing. For instance, the friction and wear performance of these biolubricants are reported in the literature [27,28], but tested in limited conditions, or in a single testing machine. Therefore, the film thickness and the lubrication regimes of CO and TCO have only been superficially explored. Besides, regarding the aminolyzed castor oil (ACO), there are no reports of its tribological performance. Only a single study was found [13], where just the physico-chemical properties of ACO are reported.

Considering the above-mentioned research gaps and issues, this work is dedicated to provide a more complete tribological description and comparison between a base vegetable oil (castor oil) with two modified biolubricants, i.e. transesterified castor oil and aminolyzed castor oil. An extensive experimental work (film thickness measurement, Stribeck curve and scuffing resistance) was performed aiming to obtain a wide database, thereby allowing a detailed investigation on the tribological performance of the biolubricants selected in this study.

## 2. Methodology

### 2.1. *Lubricants production and properties*

Three samples of lubricants were evaluated. Among the samples, one is the castor oil (CO) base itself. The others two oils were subjected to chemical processes (chemical modifications), i.e. aminolysis (ACO), and transesterification process (TCO). Transesterification is a chemical process where esters are synthesized by reacting vegetable oils or animal fats with alcohol. During the process, the alcohol reacts with the triglyceride, breaking the ester bonds and forming glycerol and fatty acid alkyl esters. Then, glycerol is removed from the reaction mixture. This process leads to the modification of the lubricant's properties, such as its viscosity, pour point, and oxidative stability [2,13,29]. Aminolysis is a chemical process which involves the conversion of triglycerides into amides. The process occurs when amines react with triglycerides, causing the triglyceride molecule to break down and then forming amides. The glycerol by-product is removed, and the purified fatty acid amides are used as biolubricant. The lubricants produced by this process can exhibit improved thermal and oxidative properties [13].

The castor oil was purchased from a commercial source (Azevedo óleos). ACO and TCO were provided by SINPOL (Laboratory of Synthesis of Polymer - Federal University of Rio Grande do Sul, Brazil). A complete chemical analysis of these three biolubricants was made, and it is described elsewhere [13]. A schematic view of the molecules structures and transformations is shown in Figure 1. CO is a triacylglycerol, while ACO and TCO have only one long alkyl chain derived from ricinoleic acid attached to an ester (TCO) or an amide group (ACO). It is also important to note that the chemical reactions used introduce new polar groups into the molecules of TCO and ACO [13]. This new polar groups are represented as the amide carbonyl (green part of the molecule, as seen in Figure 1) for the ACO and as the new hydroxyl group (red part of the molecule) for the TCO.

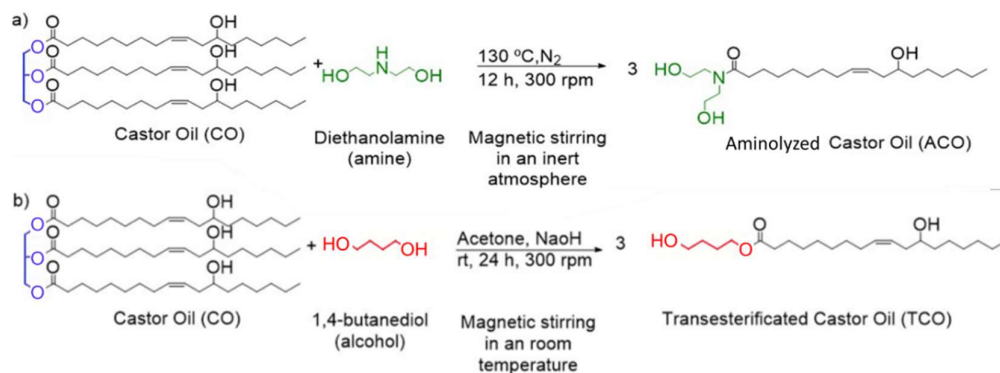


**Figure 1. Schematic of (a) aminolysis, and (b) transesterification process applied to castor oil base.**

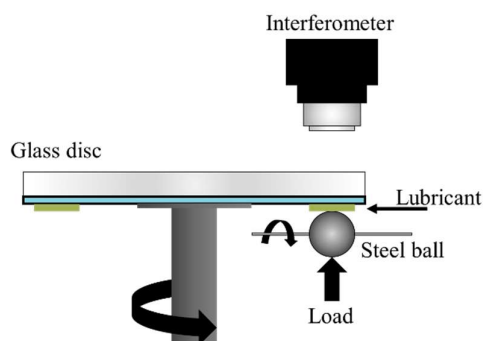
Prior to the tribological tests, physical properties (viscosity and the density) of the three biolubricants were measured. The dynamic viscosity of the three oils was determined with a rheometer ARES-G2 – TA Instruments® equipped with an Advanced Peltier System (APS). The 2° degrees 40 mm cone-plate geometry was used under a shear rate of 0.1 s<sup>-1</sup> for 300 s according to the flow ramp method. The dynamic viscosities were measured according to SAE J300 [30] at 40 and 100 °C. Additionally to this procedure, a third measurement at room temperature (27 °C) was performed. The resulting viscosities at the three temperatures as well as the densities are showed in Table 1. All the three biolubricants exhibited a reduction in dynamic viscosity as the temperature of analysis increased. Comparing the three oils, CO presents the highest values, followed by ACO and TCO.

**Table 1. Physical and rheological properties of the biolubricants.**

Sample	Dynamic viscosity [Pa·s]			Density [g/cm <sup>3</sup> ]
	27 °C	40 °C	100 °C	
CO	0.5727	0.2358	0.0192	1.0134
ACO	0.4553	0.1918	0.0164	1.0953
TCO	0.2118	0.1136	0.0119	1.0230

## 2.2. Tribological tests and film thickness measurement

An EHD2 Ultra-Thin Measurement apparatus (PCS Instruments) was used for the film thickness measurement. A 100 Cr 6 steel ball was loaded against a glass disc using a normal force of 30 N (0.56 GPa maximum Hertz pressure), with the rolling speed varying between 1.49 to 0.04 m/s in 11 acquisition steps at 27 °C. Two different slide-to-roll ratios (SRR) were evaluated, one with SRR = 0 (pure rolling) and the other with SRR = 1 (sliding and rolling), performing two repetitions per test. Figure 2 presents the scheme of the EHD2 apparatus, while Table 2 summarizes the test conditions.

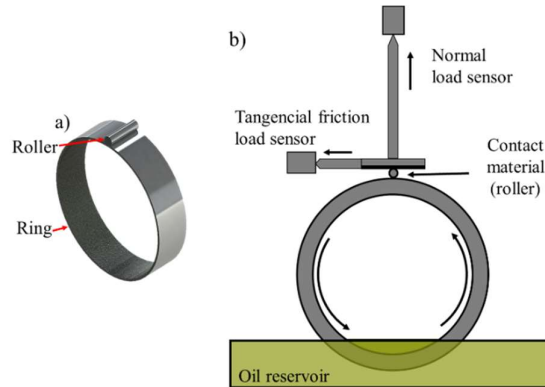


**Figure 2. Diagram of the EHD2 Ultra-Thin Measurement apparatus (PCS Instruments).**

**Table 2. Ball-on-disc test conditions for film thickness measurement.**

	Ball	Disc
Radius – $R_{x,y}$ [mm]	9.525	$\infty$
Average roughness – $R_a$ [nm]	$\cong 20$	-
Material [-]	100 Cr 6 steel	Glass
Elastic modulus – $E$ [GPa]	210	64
Poisson coefficient – $\nu$ [-]	0.3	0.2
Normal force – $F$ [N]	30	
Rolling speed – $U$ [m/s]	1.49 – 0.04	
Slide to Roll Ratio – $SRR$ [-]	0% and 100%	
Equivalent elastic modulus – $E^*$ [GPa]	51.7	
Maximum Hertz pressure – $p_h$ [GPa]	0.56	
Hertzian radius – $a$ [ $\mu\text{m}$ ]	160.61	

Other two different tribological tests were performed with the oils. The first one was a block-on-ring (BoR), where a fluid film lubrication was employed aiming to measure the Stribeck curve. For the BoR test, the diameter of the ring and the roller (used as a block) was 60 mm and 4 mm, respectively. Both the ring and roller have a length of 15.4 mm, and are made of SAE 52100. A linear contact area was assumed. A representation of the BoR specimens and their relative positions are made in Figure 3-a. Through the block-on-ring tests, the Stribeck curve of the three oils was measured. In this equipment, the normal load was applied by a mechanical actuator and monitored with a load cell and an acquisition system. The friction force was measured directly as a reaction force, and also recorded with a load cell and an acquisition system (Figure 3-b). It is worth noting the oil reservoir, which is filled with oil in order to provide a fluid film lubrication during the tests. More details of this test rig can be seen in [31]. The tests were performed with a normal force of 30 N, which results in a 153 MPa average Hertzian contact pressure. The total sliding distance was set as 188 m and the angular speeds varied as 13, 32, 80, 159, 318 and 474 rpm, corresponding in linear sliding speeds of 0.04, 0.1, 0.25, 0.5, 1.0 and 1.49 m/s respectively. Data were measured and acquired using a National, model NIUSB6009, at a sampling rate of 3 kHz. Then a moving average filter was performed and the sampling rate was reduced to 150 Hz. The mean square roughness ( $R_q$ ) of both, the ring and the roller, was measured using a Mitutoyo SJ-201, resulting in an average of  $R_q = 0.145 \pm 0.01 \mu\text{m}$  for the ring and  $R_q = 0.015 \pm 0.01 \mu\text{m}$  for the roller. An overview of the testing parameters is showed in Table 3.

**Figure 3. Block on ring apparatus: (a) representation of the specimens and (b) simplified schematic of the equipment.**

**Table 3. Parameters of the block-on-ring test.**

Sliding speed [m/s]	Rotation [rpm]	Number of revolutions [-]	Distance [m]	Time [s]	Normal force [N]	Average Hertz contact stress [MPa]
1.49	474			127		
1.00	318			188		
0.50	159	1000	188	377	30	153
0.25	80			754		
0.10	32			1885		
0.04	13			4712		

The second tribological test was a Pin-on-Disc (PoD), where a starved lubrication was used in order to determine the scuffing resistance of each oil. For this test, the disc has 55 mm in diameter, whereas the pin has a diameter of 12 mm with a spherical face with radius of 200 mm. This spherical face helps to ensure a good contact of the pin with the disc. These specimens are also made of SAE 52100 and a representation of the PoD specimens and their relative positions are made in Figure 4-a. The test was carried out in a multifunctional tribometer (Figure 4-b) developed by Neis, 2012 [32]. In this equipment, the normal force is applied by a pneumatic actuator that forces the pin against the disc for a fixed sliding distance. Using a torque transducer installed at the machine's shaft, the torque generated by friction is measured. Then, the coefficient of friction (CoF) ( $\mu$ ) is calculated through Equation (1), where the  $T_r$  is the torque,  $F_n$  is the normal force and the  $r$  is the sliding radius (radius of the contact point in the disc). A schematic view of the equipment is showed in Figure 4-b.

$$\mu = \frac{T_r}{F_n \cdot r} \quad (1)$$

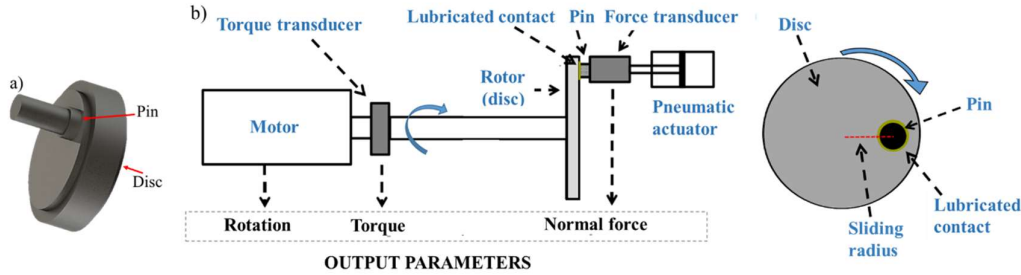


**Figure 4. Pin-on-disc setup: (a) representation of the specimens and (b) simplified diagram of the equipment.**

In order to reproduce the starved lubrication, 0.4 mL of oil was applied in the disc and pin (0.2 mL in each) prior to the pin-on-disc tests. A sliding radius of 17.5 mm was used. The initial force was set 50 N (98 MPa average Hertzian contact stress), with an increasing rate of 0.2 N/s. The test duration was one hour (3600 s), which means that the final force was 770 N (245 MPa average Hertzian contact stress). The rotation was maintained fixed at 272 rpm (sliding speed of 0.5 m/s).

To produce a uniform surface texture, the discs and the pins of the PoD were polished in a bench polisher for 1 minute using a 400 mesh sandpaper. After that, the mean square roughness ( $R_q$ ) of the discs were measured (3 measurements spaced at an angle of 120°) using a Mitutoyo SJ-201 rugosimeter. An average of  $R_q = 0.23 \pm 0.01 \mu\text{m}$  was found for the pins and discs. An overview of the testing parameters are shown in Table 4. Prior the beginning of all tests (PoD and BoR), the tribological pairs were cleaned with a solution of 90% of xylene and 10% of ethylic alcohol to ensure that the surface was free of contaminants.

**Table 4. Parameters of the pin-on-disc tests.**

Parameter	Value	Note
Angular speed [rpm]	272	Constant
Sliding speed [m/s]	0.5	Constant
Slip radius [mm]	17.5	-
Initial normal force [N]	50	Increases with the F/T
F/T (Normal force/time rate) [N/s]	0.2	-
Final normal force [N]	770	Final value [50N+0.2N/s·3600s]
Duration [s]	3600	-
Disc lubrication [mL]	0.2	Applied at the beginning of the test
Pin lubrication [mL]	0.2	Applied at the beginning of the test
Mean square roughness (Rq) of the discs [ $\mu\text{m}$ ]	0.23±0.01	-

### 3. Results and discussion

#### 3.1. Film thickness measurement and prediction

The average film thickness results and the dynamic viscosity at 27 °C for the three lubricants, are summarized in Figure 5. The dynamic viscosity values are also included aside to the graph solely for facilitating the understanding. In both SRRs, a higher dynamic viscosity corresponds to the formation of a thicker film by the lubricants. Consequently, the order of dynamic viscosity (from highest to lowest) aligns with the film thickness, namely CO, ACO and TCO. Notably, as the SRR transitions from SRR = 0 (pure rolling) to SRR = 1 (rolling and sliding), the film demonstrates a slight reduction in thickness along with an increase in temperature. This demonstrates that the form relative motion (observed through SRR) and the generated heat have influence on the film thickness [33–36]. As the sliding ratio increases from SRR=0 to SRR=1, the lubricant film becomes thinner, which is an indicative of reduced lubrication in the contact area [37,38]. It is worth noting that both the BoR and PoD tests represent pure sliding conditions, which is the worst case scenario for lubrication.

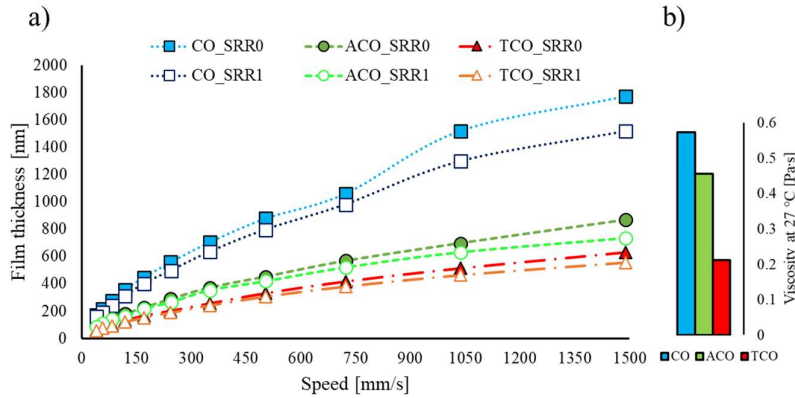


**Figure 5. Results and comparison of the average film thickness measurement tests for SRR = 0 (pure rolling) and SRR = 1 (sliding and rolling); (b) dynamic viscosity at 27 °C.**

In order to have a complete characterization of the three oils, the experimental results of film thickness with SRR = 0 were used to estimate the piezoviscosity coefficient ( $\alpha$ ) of each biolubricants. To this end, from Equation (2) proposed by Hamrock and Dowson [39], it was possible to employ the Least Squares Method to determine the best fitting value for piezoviscosity ( $\alpha$ ) ( $\text{m}^2/\text{N}$ ).

$$h_c = 2.69 \cdot R_{x,y} \cdot \left( \frac{\eta_0 \cdot u}{2E^* \cdot R_{x,y}} \right)^{0.67} \cdot (2E^* \cdot \alpha)^{0.53} \cdot \left( \frac{F}{2E^* \cdot R_{x,y}^2} \right)^{-0.067} \cdot C_0 \quad (2)$$

Where  $h_c$  is the central film thickness (m),  $R_{x,y}$  is the effective radius (m),  $\eta_0$  is the dynamic viscosity (Pa·s),  $u$  is the surface velocity (m/s),  $E^*$  is the effective elastic modulus (N/m<sup>2</sup>) and  $F$  is the force applied (N). The constant  $C_0$  in Equation (2) is equal to 0.712 for the circular contact and was also calculated according with Hamrock and Dowson [39]. It is important to mention that only values of SRR = 0 were chosen to adjust the constants to mitigate thermal effects in the adjustment. From the current analysis, it was possible to determine the piezoviscosity coefficient of each biolubricant (Table 5). CO presents the highest  $\alpha$  followed by TCO and ACO. This shows that the chemical modifications not only alter the dynamic viscosities but also influence their response to changes in pressure (i.e. piezoviscosity).

**Table 5. Piezoviscosity results for SRR = 0.**

	CO	ACO	TCO
Piezoviscosity $\alpha$ [GPa <sup>-1</sup> ]	16.41	5.69	8.08

For the purpose of validate the values obtained for piezoviscosity ( $\alpha$ ) in the SRR = 0, they were applied in the film thickness prediction to the condition of SRR = 1 and compared with the values obtained experimentally in the test. In this case, the film thickness was corrected, according to Equations (3) and (4) using the Gupta thermal parameter presented in Equation (4) [40]. This correction is necessary due to the variation of the viscosity with the temperature as the SRR changes. In Equations (3) and (4)  $h_{cT}$  represents the central film thickness thermally adjusted (m),  $\Phi_T$  is the thermal reduction factor and  $p_h$  is the Hertzian pressure (Pa).

$$h_{cT} = \Phi_T \times h_c \quad (3)$$

$$\Phi_T = \frac{1 - 13.2 \left( \frac{p_h}{2 \cdot E^*} \right) \cdot L_T^{0.42}}{1 + 0.213 \cdot L_T^{0.42} \cdot (1 + 2.23 \cdot SRR^{0.83})} \quad (4)$$

The constant  $L_T$  and the lubricant's thermal conductivity  $k_f$  (W/(m·k)) are presented in Equations (5) and (6), respectively.

$$L_T = - \left( \frac{\partial \eta_0}{\partial T} \right) \cdot \frac{U^2}{k_f} \quad (5)$$

$$k_f = \frac{0.12 \cdot (1 - 1.667 \times 10^{-4} \cdot T)}{\rho_T} \quad (6)$$

In these equations,  $U$  is the mean rolling velocity (m/s),  $T$  is the temperature (K) and  $\rho_T$  is the density of the lubricant (kg/m<sup>3</sup>).

The results from this evaluation are shown in Figure 6. As one can see, using the estimated piezoviscosity coefficients and the thermal correction, it was possible to predict the film thickness with correlations of 99.70% for CO, 99.89% for ACO and 99.94% for TCO.

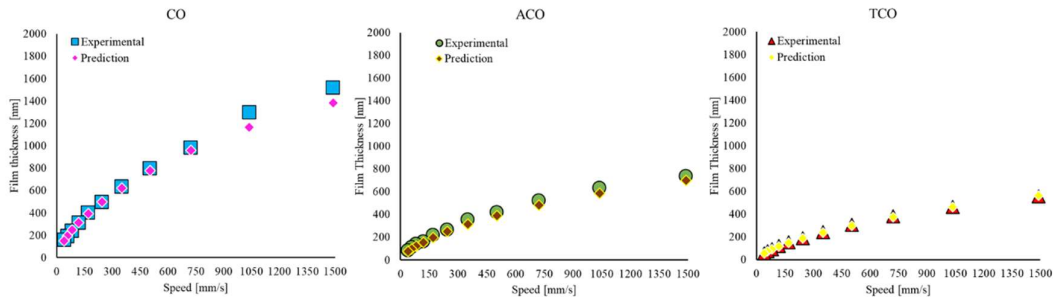


**Figure 6. Film thickness experimental measurement versus predictions ( $h_{cT}$  calculated) for each biolubricant in the SRR = 1 condition.**

In summary, the CO showed the thicker film thickness followed by ACO and TCO, which follows the same order as the dynamic viscosity. Also, it was seen that the piezoviscosity can be determined by the equation proposed by Hamrock and Dowson [39]. Besides, results from this section showed that the chemical modifications selected in this study reduced the piezoviscosity of the base vegetable oil (castor oil) in an average of 58%. The importance of piezoviscosity in the behavior of the lubricants is appointed by [41], where the authors reported that the variation of viscosity with pressure (piezoviscosity) is, in some occasions, more important than the actual values of dynamic viscosity.

### 3.2. Stribeck curve

The Stribeck curves obtained from the BoR equipment for the biolubricants are illustrated in Figure 7. The curves are plotted as a function of speed to a better distinguishment of the biolubricants. Two dashed lines are added to the graph to indicate the changes from mixed to elasto-hydrodynamic (EHD) lubrication regimes.

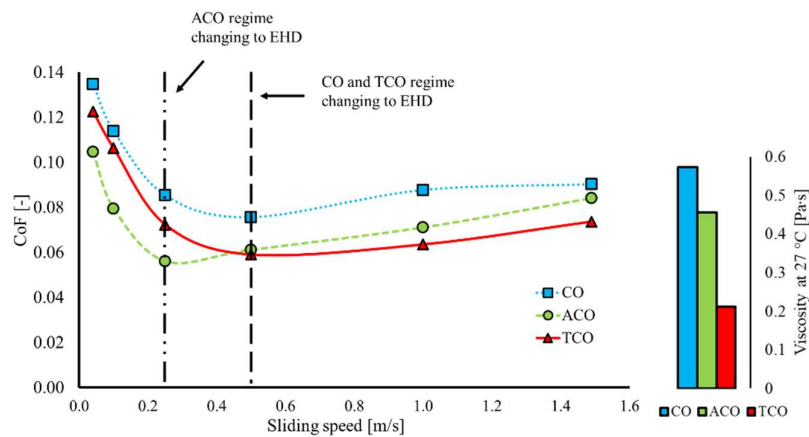


**Figure 7. Stribeck curves measured in the BoR test and viscosity in the right side.**

For higher speeds the biolubricants reach the EHD regime and the friction response is predominantly a function of the viscous behavior of the lubricant. It is important to observe that ACO reached this change in the lubrication regime a point earlier (at lower speed) than CO and TCO (these two reached the EHD regime at the same speed). So, in the EHD regime, CO exhibited the highest CoF, followed by ACO and TCO, which are in the same order than the dynamic viscosity.

When the sliding speed is reduced (in boundary and mixed lubrication regimes) the viscous behavior is not dominant, since the film thickness decreases, not being able to fully separate the asperities of the matching surfaces. In such conditions, it is interesting to note that ACO exhibited the lower value of CoF (0.104) while TCO and CO showed higher values, 0.122 and 0.135, respectively. This lower CoF of ACO towards lower sliding speeds may be due to the fact that ACO has more polar groups in its molecule (amide group, green part of the molecule, as seen in Figure 1) and therefore could have a better adsorption in the metal surface (SAE 52100). According to the literature, the adsorption is extremely important in boundary lubrication, since in this regime the lubricant is not capable of forming a hydrodynamic layer [6,42]. The adsorbed lubricant forms a strongly attached layer in the surfaces [42–44], preventing severe contact between them.

### 3.3. Scuffing resistance results

For the PoD tests, the occurrence of scuffing in the tribological pair was adopted as an end-of-test criterion. It is well known that the occurrence of scuffing is often related to the end of life of a mechanical component. Figure 8 shows typical examples of contact materials (pin and disc) that underwent scuffing (Figure 8-a and Figure 8-b), as well as contact materials where only abrasion can be seen on their surfaces (Figure 8-c and Figure 8-d).

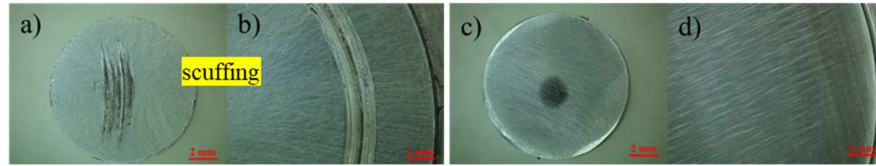


**Figure 8.** Examples of contact materials showing (a,b) scuffing and (c,d) abrasion.

From Figure 8 one can observe that scuffing is seen as a severe adhesion and can be observed macroscopically. In a test with starved lubrication, where only a very low amount of lubricant is used, the lubricant is unable to form a full film and therefore cannot reach the EHD regime [45].

Figure 9 shows the friction profile (line graphs, in the left) and the test duration (bar graphs, in the right) of all eight runs for each lubricant. The friction peaks indicate the time the lubricant film has failed and scuffing has occurred, i.e. the end of the test. Arrows are used to show the CoF magnitude when it is out of the graph scale. Moreover, the CoF curves plotted until the end of the test (3600 s) correspond to the unfailed runs. The bars lower than 3600 s (graph in the right) indicate the corresponding time where scuffing occurred.

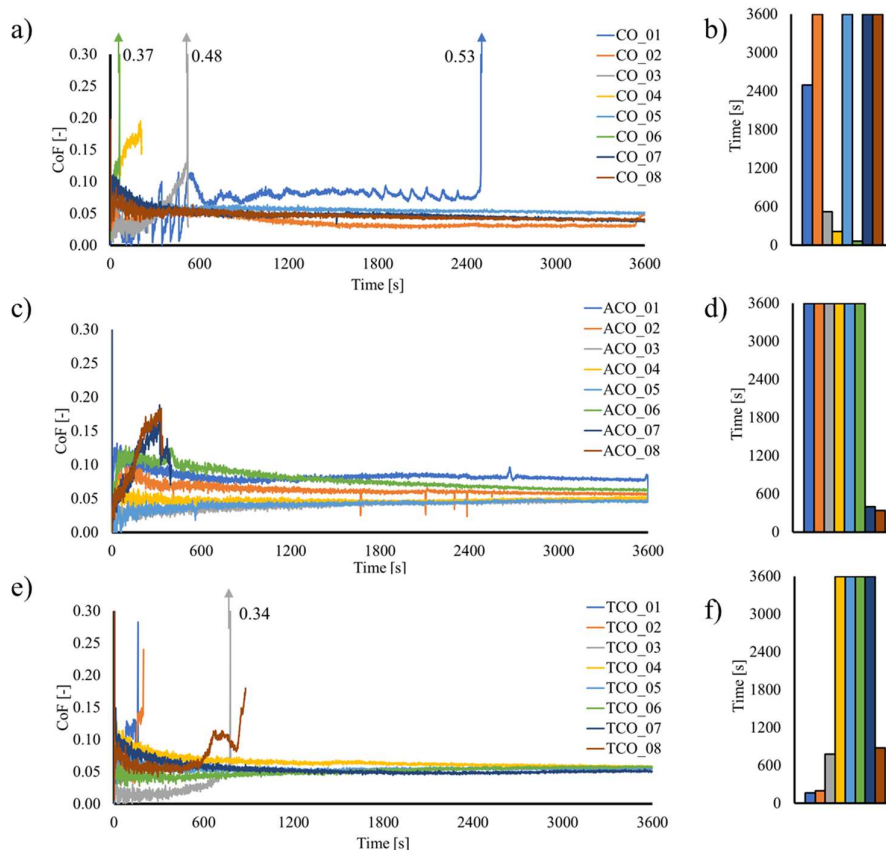


**Figure 9.** Friction profile versus time and test duration for: (a, b) CO, (c, d) ACO and (e, f) TCO.

From Figure 9-a and Figure 9-b, it can be observed that 4 out of 8 runs measured for the CO biolubricant have failed, which are seen as 4 peaks in CoF. Besides, those failures are spread along the test duration, i.e. they are widely different. Figure 9-c and Figure 9-d shows that only 2 failures out of 8 runs have occurred with ACO, which are indicated as peaks in friction during runs 07 and 08. Both failures occurred at the beginning of the test, before 400 seconds. It is also possible to see, in Figure 9-e and Figure 9-f, that TCO had 4 failures out of 8 runs. All those failures in lubrication occurred before 900 seconds.

From Figure 9, it is also noticeable that ACO showed a higher wear resistance, with 25% of the runs failing by scuffing, while both CO and TCO, had 50% of the runs resulting in scuffing failure. These results showed a good agreement with the Stribeck curve, where ACO also showed the lowest CoF in the boundary regime, meaning that the lubrication was more effective.

The main reason to explain the superior scuffing resistance of ACO involves the ability of the lubricant to adhere and maintain itself attached to the metallic surface i.e., its adsorption capacity [23,42,46,48]. Since only a small quantity of lubricant was applied to the surfaces in the PoD test, there is only a thin layer of lubricant between the metallic surfaces. This microscopic layer is the responsible for preventing direct contact between the pin and disc [23,42,48], where their desorption leads to the scuffing failure [42,46]. The better adsorption capacity of ACO may explain its superior tribological performance, which is seen through its better resistance to scuffing, as well as its reduced CoF in lower sliding speed (Stribeck curve – Figure 7). The lubricant's ability to adhere to a metallic surface is often associated with its polarity [6,48]. In case of the three biolubricants selected in this investigation, the ranking of polarity in descending order is:  $ACO > TCO > CO$ , as reported elsewhere [13]. These results are in good agreement with [49], where the lubricant (not specified by the authors) with more polar groups in its molecule showed a higher resistance to scuffing. Therefore, these properties (polarity and adsorption capacity) are especially important in boundary and mixed lubrication regimes.

Another hypothesis that might explain the better resistance to scuffing of ACO could be due to its lower value of piezoviscosity. Bowman and Stachowiak [46] reported that as the pressure in Hertzian contacts increases, due to the piezoviscosity properties, the lubricant viscosity increase almost to the point of behaving like a solid. At the same time, this increase in viscosity promotes an increase in viscous friction, therefore leading to a heating of the system, which in turns reduces the lubricant viscosity. This continues until a “critical temperature” is reached, at which point the viscosity suddenly falls, causing the lubricant film to collapse and resulting in the occurrence of the scuffing [46]. This theory was proposed by Dyson [47] and earlier was also described by Blok in a series of papers in 1973 [46]. Although the lower piezoviscosity explains the superior resistance to scuffing of ACO, the same cannot be used to explain the results of TCO and CO. In this case, there must be another reason to explain all the scuffing results, which is the polarity of the biolubricants.

#### 4. Conclusions

The present study investigated the film thickness, the piezoviscosity, the Stribeck curve and the scuffing resistance of three different variations of a biolubricant (castor oil). The following conclusions can be formulated:

- The film thickness increased with the higher dynamic viscosity. So, castor oil (CO) showed the thicker lubricant film, followed by aminolyzed castor oil (ACO) and transesterified castor oil (TCO). Also, the film thickness decreased as slide-roll ratio (SRR) changed from pure rolling ( $SRR = 0$ ) to a rolling/sliding condition ( $SRR = 1$ );
- The piezoviscosity can be estimated by the equation proposed by Hamrock and Dowson. Also, it was seen that the chemical modifications carried out in the castor oil reduced the piezoviscosity of the resulting biolubricants (ACO and TCO) in an average of 58%. The order of the estimated piezoviscosity was:  $CO > TCO > ACO$  ;
- Regarding the Stribeck test, it was seen that at higher speeds (in the elastohydrodynamic regime - EHD) the ranking of Coefficient of Friction (CoF) coincided with the order of the dynamic viscosity ( $N:CO > ACO > TCO$ ), i.e. only a viscous behavior was observed. At lower speeds (in boundary and mixed lubrication regimes) this rank changed and ACO exhibited the lowest CoF, followed by TCO and CO;

- Regarding the scuffing resistance, both CO e TCO have failed in 50% of the runs, while the ACO failed in 25% of the runs. A primary reason that could explain the superior scuffing resistance of ACO is the presence of more polar groups in its molecule. This led to a better adsorption of the lubricant on the metallic surfaces, thereby preventing direct contact between them. A secondary reason is that the lowest piezoviscosity of ACO led to lower heating in the contact region under high pressure, allowing it to keep the dynamic viscosity stable;

- Aminolysis presents as a promising chemical modification for the development of biolubricants, as it was able to reduce CoF and improve the scuffing resistance of a base vegetable oil (castor oil).

### Acknowledgements

The authors are grateful by the support of the Brazilian research agencies CNPq (Conselho Nacional de Desenvolvimento Científico e Tecnológico) and CAPES (Coordenação de Aperfeiçoamento de Pessoal de Nível Superior - Finance Code 001).

### References

- [1] W.J. Bartz, Lubricants and the environment, *Tribol. Int.* 31 (1998) 35–47. [https://doi.org/10.1016/S0301-679X\(98\)00006-1](https://doi.org/10.1016/S0301-679X(98)00006-1).
- [2] J. McNutt, Q.S. He, Development of biolubricants from vegetable oils via chemical modification, *J. Ind. Eng. Chem.* 36 (2016) 1–12. <https://doi.org/10.1016/j.jiec.2016.02.008>.
- [3] N.W.M. Zulkifli, S.S.N. Azman, M.A. Kalam, H.H. Masjuki, R. Yunus, M. Gulzar, Lubricity of bio-based lubricant derived from different chemically modified fatty acid methyl ester, *Tribol. Int.* 93 (2016) 555–562. <https://doi.org/10.1016/j.triboint.2015.03.024>.
- [4] J. Basiron, M.F. Bin Abdollah, M.I.C. Abdullah, H. Amiruddin, Lubricant mechanisms of eco-friendly lubricant blended with mineral oil for steel-steel contact, *Tribol. Int.* 186 (2023) 108653. <https://doi.org/10.1016/j.triboint.2023.108653>.
- [5] N.J. Fox, G.W. Stachowiak, Vegetable oil-based lubricants-A review of oxidation, *Tribol. Int.* 40 (2007) 1035–1046. <https://doi.org/10.1016/j.triboint.2006.10.001>.
- [6] G.W. Stachowiak, A.W. Batchelor, *Engineering tribology*, 2005. <https://doi.org/10.1017/CBO9780511805905>.
- [7] A. Adhvaryu, S.Z. Erhan, J.M. Perez, Tribological studies of thermally and chemically modified vegetable oils for use as environmentally friendly lubricants, *Wear.* 257 (2004) 359–367. <https://doi.org/10.1016/j.wear.2004.01.005>.
- [8] S. Soni, M. Agarwal, Lubricants from renewable energy sources – a review, *Green Chem. Lett. Rev.* 7 (2014) 359–382. <https://doi.org/10.1080/17518253.2014.959565>.
- [9] A.Z. Syahir, N.W.M. Zulkifli, H.H. Masjuki, M.A. Kalam, A. Alabdulkarem, M. Gulzar, L.S. Khuong, M.H. Harith, A review on bio-based lubricants and their applications, *J. Clean. Prod.* 168 (2017) 997–1016. <https://doi.org/10.1016/j.jclepro.2017.09.106>.
- [10] E.J. Parente, J.P.C. Marques, I.C. Rios, J.A. Cecilia, E. Rodríguez-Castellón, F.M.T. Luna, C.L. Cavalcante, Production of biolubricants from soybean oil: Studies for an integrated process with the current biodiesel industry, *Chem. Eng. Res. Des.* 165 (2021) 456–466. <https://doi.org/10.1016/j.cherd.2020.11.012>.
- [11] N.K. Attia, S.A. El-Mekawi, O.A. Elardy, E.A. Abdelkader, Chemical and rheological assessment of produced biolubricants from different vegetable oils, *Fuel.* 271 (2020) 117578. <https://doi.org/10.1016/j.fuel.2020.117578>.
- [12] J.A.C. da Silva, A.C. Habert, D.M.G. Freire, A potential biodegradable lubricant from castor biodiesel esters, *Lubr. Sci.* 24 (2012) 273–292. <https://doi.org/10.1002/ls.1205>.

- [13] P. Stradolini, M. Gryczak, Polyols from castor oil ( *Ricinus communis* ) and epoxidized soybean oil ( *Glycine max* ) for application as a lubricant base, *J. Am. Oil Chem. Soc.* (2023) 1–14. <https://doi.org/10.1002/aocs.12749>.
- [14] J.M. Encinar, S. Nogales-Delgado, N. Sánchez, J.F. González, Biolubricants from Rapeseed and Castor Oil Transesterification by Using Titanium Isopropoxide as a Catalyst : Production and Characterization, *Catalysts*. (2020). <https://doi.org/10.3390/catal10040366>.
- [15] Y. Ma, X. Zhu, Y. Zhang, X. Li, X. Chang, L. Shi, S. Lv, Y. Zhang, Castor oil-based adhesives : A comprehensive review, *Ind. Crop. Prod.* 209 (2024) 117924. <https://doi.org/10.1016/j.indcrop.2023.117924>.
- [16] A.G. Khiratkar, K.R. Balinge, D.S. Patle, M. Krishnamurthy, K.K. Cheralathan, P.R. Bhagat, Transesterification of castor oil using benzimidazolium based Brønsted acid ionic liquid catalyst, *Fuel*. 231 (2018) 458–467. <https://doi.org/10.1016/j.fuel.2018.05.127>.
- [17] S. Edla, A.D. Thampi, P. Prasannakumar, S. Rani, Evaluation of physicochemical, tribological and oxidative stability properties of chemically modified rice bran and karanja oils as viable lubricant base stocks for industrial applications, *Tribol. Int.* 173 (2022) 107631. <https://doi.org/10.1016/j.triboint.2022.107631>.
- [18] A. Ruggiero, R. D’Amato, M. Merola, P. Valašek, M. Müller, Tribological characterization of vegetal lubricants: Comparative experimental investigation on *Jatropha curcas* L. oil, Rapeseed Methyl Ester oil, Hydrotreated Rapeseed oil, *Tribol. Int.* 109 (2017) 529–540. <https://doi.org/10.1016/j.triboint.2017.01.030>.
- [19] C.N. Ude, C.N. Igwilo, K. Nwosu-obiogu, P.C. Nnaji, C.N. Oguanobi, N.F. Amulu, C. Nneka, U.C. Omenihu, Optimization of dual transesterification of jatropha seed oil to biolubricant using hybridized response surface methodology (RSM) and adaptive neuro fuzzy inference system (ANFIS) -genetic algorithm (GA), *Sustain. Chem. Environ.* 4 (2023) 100050. <https://doi.org/10.1016/j.scenv.2023.100050>.
- [20] I. Chakraborty, K. Chatterjee, Polymers and Composites Derived from Castor Oil as Sustainable Materials and Degradable Biomaterials: Current Status and Emerging Trends, *Biomacromolecules*. 21 (2020) 4639–4662. <https://doi.org/10.1021/acs.biomac.0c01291>.
- [21] R. Kakuchi, K. Fukasawa, L.C. Chou, H. Kim, H. Amii, Fundamental insights into aminolysis postpolymerization modification reaction of polymers featuring  $\alpha,\alpha$ -Difluoroacetate Esters, *Polymer (Guildf)*. 230 (2021). <https://doi.org/10.1016/j.polymer.2021.124058>.
- [22] Y. Abdullayev, V. Abbasov, F. Nasirov, N. Rzayeva, L. Nasibova, J. Autschbach, Computational mechanistic studies of the carbon–carbon double bond difunctionalization via epoxidation and subsequent aminolysis in vegetable oils, *Int. J. Quantum Chem.* 121 (2021) 1–7. <https://doi.org/10.1002/qua.26609>.
- [23] P.A. Bonnaud, H. Moritani, T. Kinjo, N. Sato, M. Tohyama, Improving the adsorption strength of amine-based organic additives for reducing wear, *Tribol. Int.* 187 (2023) 108675. <https://doi.org/10.1016/j.triboint.2023.108675>.
- [24] B. Liu, H. Essawy, Z. Li, G. Du, J. Liang, D. Hou, X. Zhou, J. Zhang, Facile preparation of epoxidized soybean oil-hexanediamine resin for fabrication of pressure-sensitive adhesives, *Prog. Org. Coatings*. 182 (2023) 107633. <https://doi.org/10.1016/j.porgcoat.2023.107633>.
- [25] D. Kumar, A. Ali, Direct synthesis of fatty acid alkanolamides and fatty acid alkyl esters from high free fatty acid containing triglycerides as lubricity improvers using heterogeneous catalyst, *Fuel*. 159 (2015) 845–853. <https://doi.org/10.1016/j.fuel.2015.07.046>.
- [26] H.P. Das, T.S.V.R. Neeharika, C. Sailu, V. Srikanth, T.P. Kumar, K.N.P. Rani, Kinetics of amidation of free fatty acids in jatropha oil as a prerequisite for biodiesel production, *Fuel*. 196 (2017) 169–177. <https://doi.org/10.1016/j.fuel.2017.01.096>.
- [27] R. Al Sulaimi, A. Macknoja, M. Eskandari, A. Shirani, B. Gautam, W. Park, P. Whitehead, A.P. Alonso, J.C. Sedbrook, K.D. Chapman, D. Berman, Evaluating the effects of very long chain and hydroxy fatty acid content on tribological performance and thermal oxidation behavior of plant-based lubricants, *Tribol. Int.* 185 (2023) 108576. <https://doi.org/10.1016/j.triboint.2023.108576>.

- [28] D. Kumar, A. Kumar, A. Singla, R. Dewan, Production and tribological characterization of castor based biodiesel, *Mater. Today Proc.* 46 (2021) 10942–10949. <https://doi.org/10.1016/j.matpr.2021.02.009>.
- [29] C. Murru, R. Badía-Laíño, M.E. Díaz-García, Oxidative Stability of Vegetal Oil-Based Lubricants, *ACS Sustain. Chem. Eng.* 9 (2021) 1459–1476. <https://doi.org/10.1021/acssuschemeng.0c06988>.
- [30] SAE J300, Engine Oil Classification (SAE J300), (1999).
- [31] F. Cardoso, F. Ferreira, A. Cavaleiro, A. Ramalho, Performance of diamond-like carbon coatings (produced by the innovative Ne-HiPIMS technology) under different lubrication regimes, *Wear.* 477 (2021). <https://doi.org/10.1016/j.wear.2021.203775>.
- [32] P.D. Neis, Projeto E Construção De Um Tribômetro Com Controle Independente Da Temperatura Do Disco, Universidade Federal do Rio Grande do Sul, 2012.
- [33] M. Omasta, J. Adam, P. Sperka, I. Krupka, M. Hartl, On the temperature and lubricant film thickness distribution in EHL contacts with arbitrary entrainment, *Lubricants.* 6 (2018). <https://doi.org/10.3390/lubricants6040101>.
- [34] Y. Zhao, P.L. Wong, J.H. Mao, Solving coupled boundary slip and heat transfer EHL problem under large slide–roll ratio conditions, *Tribol. Int.* 133 (2019) 73–87. <https://doi.org/10.1016/j.triboint.2019.01.013>.
- [35] Y. Waddad, V. Magnier, P. Dufrenoy, G. De Saxcé, Heat partition and surface temperature in sliding contact systems of rough surfaces, *Int. J. Heat Mass Transf.* 137 (2019) 1167–1182. <https://doi.org/10.1016/j.ijheatmasstransfer.2019.04.015>.
- [36] B.J. Hamrock, S.R. Schmid, B.O. Jacobson, *Fundamentals of Fluid Film Lubrication Second Edition*, Second, 2004.
- [37] H. Cen, A. Morina, A. Neville, Effect of slide to roll ratio on the micropitting behaviour in rolling-sliding contacts lubricated with ZDDP-containing lubricants, *Tribol. Int.* 122 (2018) 210–217. <https://doi.org/10.1016/j.triboint.2018.02.038>.
- [38] G. Amine, N. Fillot, D. Philippon, N. Devaux, J. Dufils, E. Macron, Dual experimental-numerical study of oil film thickness and friction in a wide elliptical TEHL contact: From pure rolling to opposite sliding, *Tribol. Int.* 184 (2023) 108466. <https://doi.org/10.1016/j.triboint.2023.108466>.
- [39] B.J. Hamrock, D. Dowson, Isothermal Elastohydrodynamic Lubrication of Point Contacts - 3. Fully Flooded Results., *Am. Soc. Mech. Eng.* (1976) 264–275.
- [40] P.K. Gupta, H.S. Cheng, D. Zhu, N.H. Forster, J.B. Schrand, Viscoelastic effects in MIL-L-7808-type lubricant, part I: Analytical formulation, *Tribol. Trans.* 35 (1992) 269–274. <https://doi.org/10.1080/10402009208982117>.
- [41] J.A. Brandão, M. Meheux, J.H.O. Seabra, F. Ville, M.J.D. Castro, Traction curves and rheological parameters of fully formulated gear oils, *Proc. Inst. Mech. Eng. Part J J. Eng. Tribol.* 225 (2011) 577–593. <https://doi.org/10.1177/1350650111405111>.
- [42] R. Bayat, A. Lehtovaara, Scuffing evaluation of fully formulated environmentally acceptable lubricant using barrel-on-disc technique, *Tribol. Int.* 160 (2021) 107002. <https://doi.org/10.1016/j.triboint.2021.107002>.
- [43] S.H. Hamdan, W.W.F. Chong, J.H. Ng, M.J. Ghazali, R.J.K. Wood, Influence of fatty acid methyl ester composition on tribological properties of vegetable oils and duck fat derived biodiesel, *Tribol. Int.* 113 (2017) 76–82. <https://doi.org/10.1016/j.triboint.2016.12.008>.
- [44] A. Naveira Suarez, M. Grahm, R. Pasaribu, R. Larsson, The influence of base oil polarity on the tribological performance of zinc dialkyl dithiophosphate additives, *Tribol. Int.* 43 (2010) 2268–2278. <https://doi.org/10.1016/j.triboint.2010.07.016>.
- [45] H. Liu, C. Zhu, Z. Sun, C. Song, Starved lubrication of a spur gear pair, *Tribol. Int.* 94 (2016) 52–60. <https://doi.org/10.1016/j.triboint.2015.07.030>.

- [46] W.F. Bowman, G.W. Stachowiak, A review of scuffing models, *Tribol. Lett.* 2 (1996) 113–131.  
<https://doi.org/10.1007/BF00160970>.
- [47] A. Dyson, Scuffing, *Treatise Mater. Sci. Technol.* 13 (1979) 175–216.  
[https://doi.org/10.1016/s0161-9160\(13\)70068-1](https://doi.org/10.1016/s0161-9160(13)70068-1).
- [48] J.P. Ewen, S.K. Kannam, B.D. Todd, D. Dini, Slip of Alkanes Confined between Surfactant Monolayers Adsorbed on Solid Surfaces, *Langmuir.* 34 (2018) 3864–3873.  
<https://doi.org/10.1021/acs.langmuir.8b00189>.
- [49] L. Wojciechowski, K.J. Kubiak, T.G. Mathia, Roughness and wettability of surfaces in boundary lubricated scuffing wear, *Tribol. Int.* 93 (2016) 593–601.  
<https://doi.org/10.1016/j.triboint.2015.04.013>.